Cationic and Anionic Impact on the Electronic Structure of Liquid Water

Zhong Yin,*[†,‡,+] Ludger Inhester,*[†,§,+] Sreevidya Thekku Veedu,[†,‡] Wilson Quevedo,[∥]
Annette Pietzsch,[∥] Philippe Wernet,[∥] Gerrit Groenhof,[⊥] Alexander Föhlisch,[∥,#] Helmut Grubmüller,*[‡]
and Simone Techert*[†,‡,∇]

[†]Deutsches Elektronen-Synchrotron DESY, Notkestrasse 85, 22607 Hamburg, Germany
[‡]Max Planck Institute for Biophysical Chemistry, Am Fassberg 11, 37077 Göttingen, Germany
[§]Center for Free-Electron Laser Science, Notkestrasse 85, 22607 Hamburg, Germany
[∥]Helmholtz-Zentrum Berlin GmbH, Albert-Einstein-Strasse 15, 12489 Berlin, Germany
[⊥]University of Jyväskylä, P.O. Box 35, 40014 Jyväskylä, Finland
[#]University of Potsdam, Karl-Liebknecht-Strasse 24-25, 14476 Potsdam, Germany
[∇]University of Göttingen, Friedrich-Hund-Platz 1, 37077 Göttingen, Germany

S *Supporting Information*

ABSTRACT: Hydration shells around ions are crucial for many fundamental biological and chemical processes. Their local physicochemical properties are quite different from those of bulk water and hard to probe experimentally. We address this problem by combining soft X-ray spectroscopy using a liquid jet and molecular dynamics (MD) simulations together with ab initio electronic structure calculations to elucidate the water−ion interaction in a $MgCl_2$ solution at the molecular level. Our results reveal that salt ions mainly affect the electronic properties of water molecules in close vicinity and that the oxygen K-edge X-ray emission spectrum of water molecules in the first solvation shell differs significantly from that of bulk water. Ion-specific effects are identified by fingerprint features in the water X-ray emission spectra. While Mg^{2+} ions cause a bathochromic shift of the water lone pair orbital, the 3p orbital of the Cl^- ions causes an additional peak in the water emission spectrum at around 528 eV.
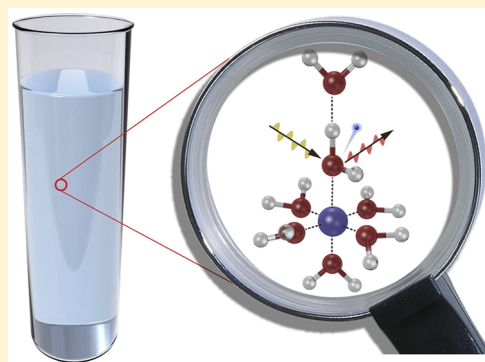
Aqueous solutions are ubiquitous in nature and play an important role for a wide range of biological, environmental, and chemical processes.[1−3] The solvation of water molecules around ions is of particular interest because it determines the fundamental mechanisms and dynamics of many chemical and biological systems.[4−6] Ion-induced changes include, among others, distortion of the electronic properties as well as geometrical arrangements of water molecules. A considerable number of experiments have been performed to elucidate the water−ion interaction, and interpretations of the data suggest sometimes a complex picture about the nature of the ion solvation.[7−24] Studies from X-ray scattering,[7] dielectric relaxations,[8,9] time-resolved IR,[10−13] NMR,[14] and terahertz spectroscopy[15] showed that the impact on water molecules by solvated ions is mainly restricted to water molecules in close vicinity to the ion. Only for specific combinations of strongly hydrated salt ions has it been reported that the impact on the orientation of water molecules may extend beyond the first solvation shell.[10] Nevertheless, neutron scattering studies revealed that the oxygen−oxygen radial distribution function is altered by NaCl and KCl solutes beyond the first solvation

shell.[16] The seemingly contradicting results may be due to the sensitivity of the utilized methods to different properties of the aqueous solutions. While neutron scattering probes the average of the overall structure, ultrafast IR spectroscopy, for example, is sensitive to the dynamical properties of water.

Because the electronic properties of the water molecules are sensitive to their chemical environment, probing them may elucidate further information about the hydrogen bond (HB) structure. X-ray spectroscopy allows direct measurement of the electronic properties of a system and provides direct information about the local electronic structure around a specific element in a bulk chemical environment.[25−40]

Previous soft X-ray absorption (XA) studies on aqueous solutions reported strong distortions of the pre-, main, and post-edge of the XA spectra on the oxygen K-edge in the vicinity of the ions.[7,30,31,33] These changes have been assigned

to weakening and strengthening of the HBs in the solvation shell around the cations.[7,30−33]

Complementary information to XA spectroscopy is gained from X-ray emission spectroscopy (XES). XES probes the valence electrons, which are essential for chemical bonding. The X-ray emission (XE) spectrum of water shows three prominent features[27] that are attributed to the three outer valence orbitals of water, the lone pair orbital $1b_1$ at ∼526 eV, and the internal bonding orbitals $3a_1$ at ∼524 eV and $1b_2$ at ∼521 eV. Experiments with higher energy resolution revealed additionally a splitting of the lone pair orbital contribution into two parts and further showed the sensitivity of this lone pair orbital fine structure to the HB environment based on temperature and isotope measurements.[35,36]

Yet, the origin of the splitting has stirred a discussion about the nature of the fine structure. Mainly two models have been suggested to explain this effect: The fine structure arises either (1) from nuclear dynamics during the core hole lifetime[35,41] or (2) from two different structural motifs.[36] In model (1), the higher-energy peak arises from intact water molecules, and the lower-energy peak is from ultrafast proton transfer facilitated by intact HBs.[34] In model (2), the lower peak is from water molecules in a fully hydrogen-bonded tetrahedral coordination, while the higher-energy peak stems from water molecules in a strongly distorted HB configuration.[36] Despite this controversy, there is consensus that the XE spectrum of water on the oxygen K-edge is a fingerprint of the HB network.[27,35,36]

Recently, several soft XES experiments have reported that the electronic properties of water are altered by the presence of salt ions only at high salt concentrations.[28,37−40] However, the dominating change that is observed is an intensity decrease of the lower-energy part of the split lone pair orbital peak in dependence of the concentration and the type of salt ions, which consisted mainly of Cl^- as the anion and various cations (NH_4^+, Li^+, K^+, Na^+, Mg^{2+} and Ca^{2+}). These changes were assigned to distortion of the HB network.[28,37−40] Modifications in the electronic properties were relatively small, such that even at the highest concentration for monovalent (7 M) and divalent (4 M for $CaCl_2$) salt ions the splitting was still observed.

The changes were assigned to the impact of the cations by comparing various cations with the same Cl^- concentration.[28,40]

Jeyachandran et al.[37] introduced a three-component fit based on water model (1) and assigned one component to water molecules in the first solvation shell. Recently, the same authors also studied KBr, KCl, $MgCl_2$, and $CaCl_2$ at various concentrations and observed in highly concentrated (>3 M) solution a stronger increase of the extracted component for the Br^- anion than the Cl^- anion.[39] Additionally, this component of $MgCl_2$ and $CaCl_2$ solutions was twice as strong as that for monovalent salt solutions. Therefore, they concluded that this component represents the first hydration shell around anions. However, because of the higher charge of divalent cations compared to the monovalent cations, it is also conceivable that the increase of the additional component is due to the contribution by water molecules in the first solvation shell of the divalent cations.

The aim of the present study is therefore to elucidate the nature of ion−water interactions and its effect on the electronic properties of water using a combined study of soft X-ray spectroscopy with ab initio electronic structure calculation on aqueous solutions. We address the question how salt ions change the electronic properties of liquid water and reveal the

origin of the previously observed additional peak at ∼528 eV. To that end, we investigate the impact of salt ions in highly concentrated $MgCl_2$ solutions. Compared to monovalent cations like sodium or potassium, magnesium is divalent, and one expects a stronger interaction with the surrounding water molecules. Also, Mg^{2+} has a markedly shorter ion−water distance than Ca^{2+}.[42]

Figure 1 shows the XE spectra of the 4 M $MgCl_2$ solution compared to pure water. The excitation energy was set at a
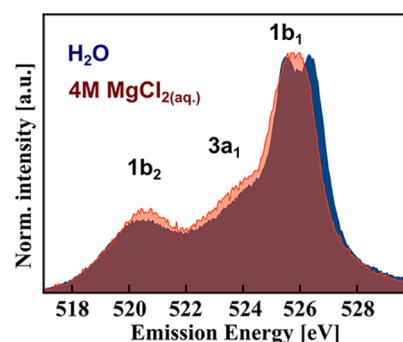

Figure 1. XE spectra of pure water in comparison with 4 M $MgCl_{2(aq)}$ solutions on the oxygen K-edge are shown.

nonresonant energy above the post-edge according to the XAS results; see the SI. They have been area-normalized for an accurate comparison of relative intensities.

For pure water (blue), three regions can be distinguished, as described in the introduction. The lone pair peak shows a double-peak structure in the pure water spectrum, in agreement with previous results.[35,36] For the 4 M solution, the intensity of the bonding orbitals $1b_2$ and $3a_1$ in $MgCl_2$ solution is more pronounced.

In contrast to the splitting in the lone pair region of pure water, for the 4 M salt solution (red), only one peak is seen. Further, this $1b_1$ peak is shifted to lower energies and to a position between the peaks of the lone pair orbital for the pure water spectrum, while the position of the other contributions is rather similar.

In previous works, no strong effects on the water's valence electronic configuration have been observed for 2 M $MgCl_2$ and $CaCl_2$ solutions with concentrations up to 4 M,[39] which contain the same number of Cl^- anions as in our 4 M $MgCl_2$ solution. The differences from previous studies are most likely due to the lower concentration (2 vs 4 M) and the different cation because Mg^{2+} has a much tighter hydration shell than the Ca^{2+} cation.[42]

Given the fact that former studies (experimental and theoretical) show a negligible effect of Cl^- ions on the electronic structure of water, even for very high concentrations,[7,24,28,30,32,33,40] we assume the number of water molecules in direct contact with Mg^{2+} ions can explain most of the salt-induced spectral changes in our 4 M solution. Accordingly, we expect the major effects of salt on the electronic properties to be understood to first approximation from the electronic configuration of the water molecules in the first solvation shell around the Mg^{2+} ion. On the basis of this additional idea, we consider the solution spectrum of the valence electronic states of water $f(E)$ to be a linear combination of the spectra arising from water molecules in the first solvation shell around Mg^{2+}, $f_{Mg}(E)$, and those arising from water molecules not in direct contact with Mg^{2+}, contributing to the spectrum of bulk water, $f_{bulk}(E)$. Referring

to the above arguments, we assume that the XE spectrum of water molecules close to Cl⁻ anions is similar to the XE spectrum of bulk water, such that the 4 M MgCl$_2$ spectrum is given by $f(E) = \alpha f_{Mg}(E) + (1 - \alpha)f_{bulk}(E)$.

From the measured spectrum $f(E)$, we thus obtain a good approximation for the isolated spectrum of water molecules in the first solvation shell of Mg^{2+}, $f_{Mg}(E) = \frac{1}{\alpha}(f(E) - (1 - \alpha)f_{bulk}(E))$, by taking the weighted difference of measured bulk water and solution spectra. The coefficient α is determined from the relative number of water molecules in the first solvation shell of Mg^{2+}. At a 4 M concentration, there are ∼13 water molecules per MgCl$_2$ salt moiety. Even at this high concentration, direct ion pairing is unlikely,[43] but there might be a relevant quantity of water molecules in direct contact with both ions. Because we ignore for the moment the impact of Cl⁻ ions altogether, we assume them to contribute to the spectrum like the water molecules in direct contact with a Mg^{2+} ion only. Considering the coordination number for Mg^{2+}, which is 6,[44] results in $\alpha = 6/13 \approx 0.46$. Figure 2 shows the resulting spectrum, now
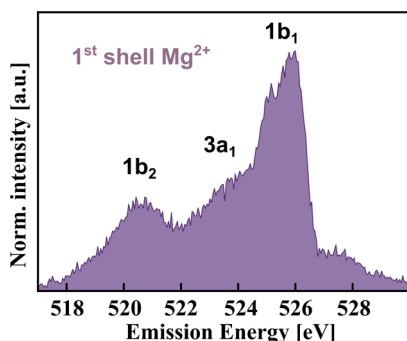

Figure 2. The difference spectrum between 4 M MgCl$_2$ and pure water is displayed. The difference represents the first hydration shell of water molecules around Mg^{2+}.

dominated by the signal from water molecules in the first shell around Mg^{2+}. The difference spectrum shows two pronounced peaks 1b$_1$ and 1b$_2$ and a broad peak between them, corresponding to the three outer valence orbital contributions. No clear splitting is observed in the lone pair region. Further, an additional shoulder appears at ∼528 eV. This difference spectrum looks very similar to the new component extracted from the water model (1) reported in ref 37.

To explain the energy shifts and the additional shoulder at ∼528 eV, we compare these experimental results to ab initio electronic structure calculations on water clusters sampled from MD simulations with and without ions. To address the question to which distances the electronic properties of water are influenced by the ions, we calculate spectra for a very dilute solutions and inspect the spectra stemming from the different solvation shells around the ions. The comparison with the experimental difference spectrum at high salt concentration requires the additional assumption that the structure of the Mg^{2+} solvation shells is mainly unaffected by the MgCl$_2$ concentration.

In Figure 3(I,II), we compare the first solvation shell spectrum with pure water. A bathochromic shift (∼0.4 eV) in the spectrum for the 1b$_1$ orbital can be observed. Figure 3(III–VI) shows the calculated fluorescence spectrum after core ionization for pure water (III) and for water in the first (IV)
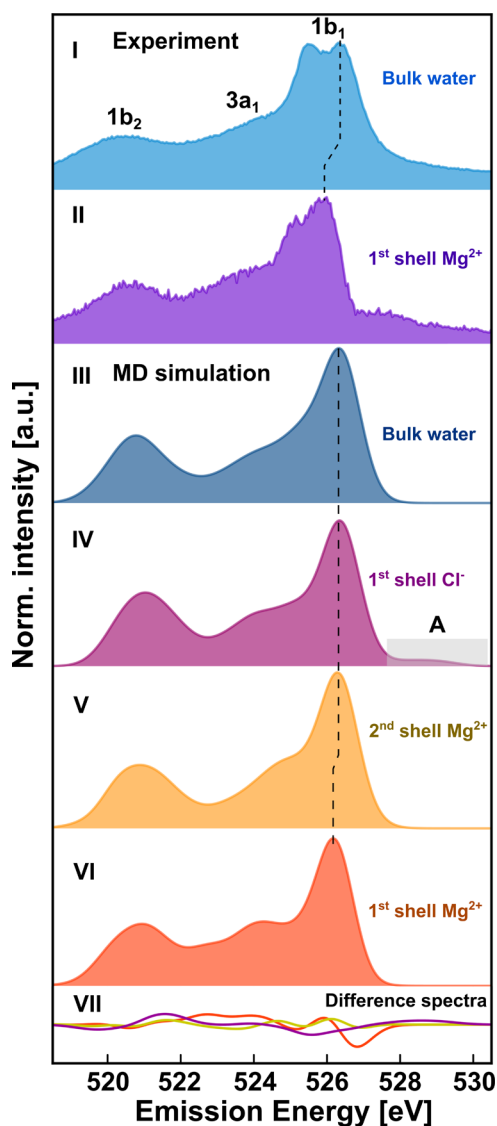

Figure 3. Ab initio spectra of (I–III) pure water clusters compared with the (VI) first and (V) second solvation shells of water around Mg^{2+} and the (IV) first shell around Cl⁻ ions with experimental results of pure water and the first around the Mg^{2+} ion. The dashed line is a guide to the eye to illustrate the shift of the 1b$_1$ peak position. Tier (VII) shows the color-coded difference spectra of the solvation shells to bulk water for the theoretical results.

solvation shell of Cl⁻ and second (V) and first (VI) hydration shells of Mg^{2+}. These are compared to the experimental results of pure water (I) and the measured difference spectrum corresponding to the first (II) shell of Mg^{2+}.

As can be seen, the calculation reproduces the different 1b$_1$, 3a$_1$, and 1b$_2$ orbital contributions that are seen in the measured spectrum. The split peak of the 1b$_1$ part is not reproduced by the calculation. As discussed before, this feature might stem from proton dynamics during the core hole lifetime[41] that are not included in our calculation. Alternatively, the fine structure might stem from two different structural motifs in the local HB structure. However, in our calculation, these structural motifs may not be correctly reproduced by the utilized force field approach. Therefore, we cannot give a satisfactory answer on the origin of the peak splitting. Apart from this discrepancy, we think that the calculation shows overall good agreement with

the measured spectrum, which allows us to understand the qualitative salt-induced changes.

For the fluorescence spectrum of the salt solution, we classify the calculated fluorescence spectrum for water molecules ionized in the first and second solvation shells of Mg^{2+} and the first solvation shell around Cl^-. Thus, we can identify the impact of the ions on the fluorescence spectrum as a function of the distance to the different ions. As can be seen, for all of the different water molecule classes, the $1b_2$ and $3a_1$ orbital contributions are rather unaffected. For the first hydration shell (IV) around Cl^- and the second solvation shell (V) around Mg^{2+}, the calculated spectrum is very similar to the calculated pure water spectrum, whereas in the first solvation shell (VI) around the Mg^{2+} ions, the $1b_1$ orbital contribution is red-shifted, which is also mirrored in the difference spectra in tier (VII). In the difference spectra, noticeable changes in the second solvation shell around the Mg^{2+} are observed. However, they are much weaker compared to the first solvation shell modifications. The red shift can be explained by the Mg^{2+}-induced polarization changes of water molecules. The lone pair orbital points toward the cation such that the electrostatic interaction between the water molecules and the Mg^{2+} cation lowers the energy of the lone pair orbital and hence lowers the emitted photon energy for reoccupation of the core hole from this orbital.

For the fluorescence spectrum of the water molecules in proximity to Cl^- ions, we see an additional shoulder above 528 eV; see tier (IV) A in Figure 3. This additional contribution was reported in a previous calculation[45] and has also been observed before in the three-component spectra fit of the aqueous solution spectrum based on the water model (1).[37] Closer inspection of the electronic structure reveals that this fluorescence signal stems from a molecular orbital representing the 3p shell of Cl^- with a slight contribution in the valence orbitals of the ionized water molecules. We can therefore assign it to refilling of the oxygen core vacancy from the Cl^- anion.

Taken together, our calculations show that, indeed, Mg^{2+} affects mainly the electronic properties of water molecules in close proximity. Whereas the water molecules close to Mg^{2+} ions have a bathochromic $1b_1$ shift, water molecules close to Cl^- show more or less an undistorted pure water XE spectrum augmented by an additional shoulder at 528 eV. Therefore, the additional shoulder in the experimental difference spectrum at ~528 eV, which we in Figure 3 tentatively assigned to the first solvation shell of Mg^{2+}, must be attributed to the water molecules in the vicinity of Cl^- anions.

In the comparison, we assumed that the solvation structure around Mg^{2+} is independent of the salt concentration. However, for the high salt concentration investigated here, it is conceivable that water molecules are in direct contact with a Mg^{2+} and Cl^- ion. Considering that the overall ion impact on the XE spectra is rather small, we speculate that the ion's impact is additive, and in this case, a water molecule may show both ion-induced features; for further discussion, see the SI.

In experimental XE studies, noticeable distortion in the electronic properties of water is only observed at high salt concentration.[28,37−39] Theoretical results show significant changes in the electronic properties of water molecules in proximity of the ions. For water molecules in the second solvation shell of the ion and beyond, the electronic properties of water show negligible distortions compared to bulk water. On the basis of these facts, we conclude that ions mainly influence the electronic properties of water molecules in close

vicinity. Soft XES is therefore particularly sensitive to the local environment of the ion and less sensitive to the geometrical arrangement of water molecules in the bulk far from the ion.

In summary, we compared the XE spectrum of a 4 M $MgCl_2$ solution with that of pure water and revealed significant differences in the electronic properties of water. Results from ab initio electronic structure calculations agree with our experimental findings, except for the fine structure of the $1b_1$ peak region, which is likely due to the lack of explicit core hole excited-state dynamics in the spectra calculations.[41] Because of this agreement, the simulation results serve to explain the observed differences in terms of a microscopic model. Accordingly, it is mainly the water molecules in the immediate vicinity of the salt ions whose electronic properties are markedly affected, thereby defining the sensitivity of our probe.

Our results show that salt ions have indeed a significant impact on the electronic properties and that cations and anions have an ion-specific influence on the electronic states of water, such that anionic and cationic effects leave different fingerprints on the XE spectra. The interaction of the first solvation shell water molecules with Cl^- anions leads to an additional signal at ~528 eV. In the first solvation shell around the Mg^{2+} ion, the lone pair orbital of water is bathochromatically shifted. Furthermore, the origin of the specific ion effects can be explained by Mg^{2+} cation-induced polarization changes in water and contributions of the 3p shell of Cl^- anions.

We think that the combination of soft X-ray spectroscopy with MD sampled ab initio electronic structure calculations developed and demonstrated here can serve to probe molecular interaction in a broad range of different condensed matter systems, including highly complex biomolecular structures.

■ EXPERIMENTAL AND SIMULATION METHODS

The experiments were performed at beamline U41 of the BESSY II synchrotron at Helmholtz Zentrum Berlin using the FlexRIXS endstation[46] and at P04 of PETRA III using the ChemRIXS[47] setup. For excitation, a monochromatic soft X-ray beam was utilized. The $MgCl_2$ solution was prepared from >99.0% $MgCl_2 \cdot 6H_2O$ (magnesium chloride hexahydrate) from Sigma-Aldrich at least 24 h prior to the experiment. The nonresonant excitation energies were selected from the XA spectra of water and aqueous solutions recorded in the total fluorescence yield mode; see the SI. XA and XE spectra of pure water were recorded periodically to confirm the stability of the setup; see the SI. The resolution of the spectrometer was ~0.4 at 530 eV (oxygen K-edge). The elastic peaks were used for energy calibration.

To perform ab initio calculation of the XE spectrum of liquids, we sampled molecular geometries from MD calculations. The MD calculations were conducted using the GROMACS 4.5.5 program[48] employing the Particle-Mesh-Ewald method (r_cutoff = 0.85 nm, Fourier spacing = 0.12 nm) with Nosé−Hoover temperature coupling (τ = 0.1 ps) and Parinello−Rahman pressure coupling (τ = 4.0 ps). The flexible Fergusson force field[49] was used with a time step of 0.5 fs. For pure water, we performed a 100 ps MD simulation of a box containing 1410 water molecule at a temperature of 300 K and a pressure of 10^5 Pa.

Because we expect the impact of the ions to be restricted to the first solvation shells, we performed simulations at low salt concentration. The same setup as that before was used to conduct 100 ps MD simulations for a box containing 1426 water molecules with a single Mg^{2+} ion and two Cl^- ions. The

interaction of the ions with the water molecules was described using the GROMOS45a3 force field.[50] For a discussion of the validity utilizing this force field approach, see the SI. From these MD simulations, water molecules were randomly picked at different snapshots to sample the local environment around the ionized water molecule. For the calculations of the XE spectrum, clusters around the ionized water molecule were constructed that include neighboring water molecules (oxygen−oxygen distance smaller than 3.5 Å) and neighboring ions (oxygen−ion distance smaller than 4 Å). These clusters were considered explicitly in the electronic structure calculations, while molecules and ions within a sphere of 10 Å around the ionized oxygen were included as point charges in the electronic structure calculations via electrostatic embedding.

For each of these molecule clusters, restricted Hartree−Fock orbitals with localized core orbitals were calculated employing a 6-31G(d)[51] basis set using the PSI3 electronic structure package.[52] Using this orbital set, the initial core ionized electronic state Ψ_i was described using a configuration interaction (CI) calculation involving all configurations with single excitations from the water valence orbitals into virtual orbitals, while the core hole orbital on the core ionized oxygen atom was kept singly occupied. The final valence-ionized state was described using a CI calculation involving all possible valence orbital vacancies and a reoccupied core orbital. From these CI solutions, the transition rate for fluorescence was evaluated from

$$I_0 = \frac{4}{3}\alpha^3\omega^3 \sum_{j=x,y,z} |\langle\Psi_i|d_j|\Psi_f\rangle|^2$$

where d is the dipole moment operator and $\omega = E_i - E_f$, with E_f and E_i being the final and initial state energies from the CI solutions, respectively. Finally, the obtained fluorescence line spectrum was convoluted with a Gaussian function of 1 eV fwhm to account for vibrational broadening effects and accumulated for the various water clusters. To distinguish the different chemical effects, the XE spectra were assembled for water molecules in different chemical environments. For water molecules in the first solvation shell around Mg^{2+}, Cl^-, and for water molecules in the second solvation shell of Mg^{2+}, as well as for water molecules stemming from the neat water simulation, the XE spectrum was assembled from ∼80 different water clusters.

All calculated spectra were shifted by 0.2 eV to lower energies for a better comparison with the experimental spectra.

ASSOCIATED CONTENT

Supporting Information
The Supporting Information is available free of charge on the ACS Publications website at DOI: 10.1021/acs.jpclett.7b01392.

> Additional experimental and theoretical data as mentioned in the text (PDF)

AUTHOR INFORMATION

Corresponding Authors
*E-mail: zhong.yin@desy.de (Z.Y.).
*E-mail: ludger.inhester@desy.de (L.I.).
*E-mail: hgrubmu@gwdg.de (H.G.).
*E-mail: simone.techert@desy.de (S.T.).

ORCID
Zhong Yin: 0000-0001-5594-9879
Ludger Inhester: 0000-0003-1417-4151
Philippe Wernet: 0000-0001-7011-9072
Gerrit Groenhof: 0000-0001-8148-5334

ACKNOWLEDGMENTS

REFERENCES

(1) Bakker, H. J. Structural Dynamics of Aqueous Salt Solutions. *Chem. Rev.* **2008**, *108*, 1456−1473.

(2) Hayes, R.; Warr, G. G.; Atkin, R. Structure and Nanostructure in Ionic Liquids. *Chem. Rev.* **2015**, *115*, 6357−6426.

(3) Jungwirth, P.; Tobias, D. J. Specific Ion Effects at the Air/water Interface. *Chem. Rev.* **2006**, *106*, 1259−1281.

(4) Lo Nostro, P.; Ninham, B. W. Hofmeister Phenomena: An Update on Ion Specificity in Biology. *Chem. Rev.* **2012**, *112*, 2286−2322.

(5) Ebbinghaus, S.; Kim, S. J.; Heyden, M.; Yu, X.; Heugen, U.; Gruebele, M.; Leitner, D. M.; Havenith, M. An Extended Dynamical Hydration Shell around Proteins. *Proc. Natl. Acad. Sci. U. S. A.* **2007**, *104*, 20749−20752.

(6) Alexander, R. T.; Hoenderop, J. G.; Bindels, R. J. Molecular Determinants of Magnesium Homeostasis: Insights from Human Disease. *J. Am. Soc. Nephrol.* **2008**, *19*, 1451−1458.

(7) Waluyo, I.; Huang, C.; Nordlund, D.; Bergmann, U.; Weiss, T. M.; Pettersson, L. G. M.; Nilsson, A. The Structure of Water in the Hydration Shell of Cations from X-ray Raman and Small Angle X-ray Scattering Measurements. *J. Chem. Phys.* **2011**, *134*, 064513.

(8) Wachter, W.; Fernandez, S.; Buchner, R.; Hefter, G. Ion Association and Hydration in Aqueous Solutions of LiCl and Li2SO4 by Dielectric Spectroscopy. *J. Phys. Chem. B* **2007**, *111*, 9010−9017.

(9) Rahman, H. M. A.; Hefter, G.; Buchner, R. Hydration of Formate and Acetate Ions by Dielectric Relaxation Spectroscopy. *J. Phys. Chem. B* **2012**, *116*, 314−323.

(10) Tielrooij, K. J.; Garcia-Araez, N.; Bonn, M.; Bakker, H. J. Cooperativity in Ion Hydration. *Science* **2010**, *328*, 1006−1009.

(11) Omta, A. W.; Kropman, M. F.; Woutersen, S.; Bakker, H. J. Negligible Effect of Ions on the Hydrogen-Bond Structure in Liquid Water. *Science (Washington, DC, U. S.)* **2003**, *301*, 347−349.

(12) Kropman, M. F.; Bakker, H. J. Vibrational Relaxation of Liquid Water in Ionic Solvation Shells. *Chem. Phys. Lett.* **2003**, *370*, 741−746.

(13) Park, S.; Odelius, M.; Gaffney, K. J. Ultrafast Dynamics of Hydrogen Bond Exchange in Aqueous Ionic Solutions. *J. Phys. Chem. B* **2009**, *113*, 7825−7835.

(14) Struis, R. P. W. L.; De Bleijser, J.; Leyte, J. C. 25Mg2+ and 35Cl− Quadrupolar Relaxation in Aqueous MgCl2 Solutions at 25 °C. 2. Relaxation at Finite MgCl2 Concentrations. *J. Phys. Chem.* **1989**, *93*, 7943−7952.

(15) Funkner, S.; Niehues, G.; Schmidt, D. A.; Heyden, M.; Schwaab, G.; Callahan, K. M.; Tobias, D. J.; Havenith, M. Watching the Low-Frequency Motions in Aqueous Salt Solutions: The Terahertz

Vibrational Signatures of Hydrated Ions. *J. Am. Chem. Soc.* **2012**, *134*, 1030−1035.

(16) Mancinelli, R.; Botti, A.; Bruni, F.; Ricci, M. A.; Soper, A. K. Hydration of Sodium, Potassium, and Chloride Ions in Solution and the Concept of Structure Maker/breaker. *J. Phys. Chem. B* **2007**, *111*, 13570−13577.

(17) Winter, B.; Aziz, E. F.; Ottosson, N.; Faubel, M.; Kosugi, N.; Hertel, I. V. Electron Dynamics in Charge-Transfer-to-Solvent States of Aqueous Chloride Revealed by Cl- 2p Resonant Auger-Electron Spectroscopy. *J. Am. Chem. Soc.* **2008**, *130*, 7130−7138.

(18) Jungwirth, P.; Tobias, D. J. Chloride Anion on Aqueous Clusters, at the Air-Water Interface, and in Liquid Water: Solvent Effects on Cl-Polarizability. *J. Phys. Chem. A* **2002**, *106*, 379−383.

(19) Xie, W. J.; Gao, Y. Q. A Simple Theory for the Hofmeister Series. *J. Phys. Chem. Lett.* **2013**, *4*, 4247−4252.

(20) Zhang, R.; Zhuang, W. Cation Effect in the Ionic Solution Optical Kerr Effect Measurements: A Simulation Study. *J. Chem. Phys.* **2014**, *140*, 054507.

(21) Zhang, Y.; Cremer, P. S. The Inverse and Direct Hofmeister Series for Lysozyme. *Proc. Natl. Acad. Sci. U. S. A.* **2009**, *106*, 15249−15253.

(22) Marcus, Y. The Effect of Complex Anions on the Structure of Water. *J. Solution Chem.* **2015**, *44*, 2258−2265.

(23) Chen, Y.; Okur, H. I.; Gomopoulos, N.; Macias-Romero, C.; Cremer, P. S.; Petersen, P. B.; Tocci, G.; Wilkins, D. M.; Liang, C.; Ceriotti, M.; et al. SI - Electrolytes Induce Long-Range Orientational Order and Free Energy Changes in the H-Bond Network of Bulk Water. *Sci. Adv.* **2016**, *2*, e1501891−e1501891.

(24) Gaiduk, A. P.; Galli, G. Local and Global Effects of Dissolved Sodium Chloride on the Structure of Water. *J. Phys. Chem. Lett.* **2017**, *8*, 1496−1502.

(25) de Groot, F. M. F. Multiplet Effects in X-ray Spectroscopy. *Coord. Chem. Rev.* **2005**, *249*, 31−63.

(26) Stöhr, J. *NEXAFS Spectroscopy*; Springer: Berlin, Germany, 1991.

(27) Guo, J.-H.; Luo, Y.; Augustsson, a.; Rubensson, J.-E.; Såthe, C.; Ågren, H.; Siegbahn, H.; Nordgren, J. X-ray Emission Spectroscopy of Hydrogen Bonding and Electronic Structure of Liquid Water. *Phys. Rev. Lett.* **2002**, *89*, 1−4.

(28) Yin, Z.; Rajkovic, I.; Kubicek, K.; Quevedo, W.; Pietzsch, A.; Wernet, P.; Föhlisch, A.; Techert, S. Probing the Hofmeister Effect with Ultrafast Core−Hole Spectroscopy. *J. Phys. Chem. B* **2014**, *118*, 9398−9403.

(29) Wernet, P.; Nordlund, D.; Bergmann, U.; Cavalleri, M.; Odelius, M.; Ogasawara, H.; Näslund, L. A.; Hirsch, T. K.; Ojamäe, L.; Glatzel, P.; et al. The Structure of the First Coordination Shell in Liquid Water. *Science* **2004**, *304*, 995−999.

(30) Näslund, L.-A.; Edwards, D. C.; Wernet, P.; Bergmann, U.; Ogasawara, H.; Pettersson, L. G. M.; Myneni, S.; Nilsson, A. X-Ray Absorption Spectroscopy Study of the Hydrogen Bond Network in the Bulk Water of Aqueous Solutions. *J. Phys. Chem. A* **2005**, *109*, 5995−6002.

(31) Cappa, C. D.; Smith, J. D.; Wilson, K. R.; Messer, B. M.; Gilles, M. K.; Cohen, R. C.; Saykally, R. J. Effects of Alkali Metal Halide Salts on the Hydrogen Bond Network of Liquid Water. *J. Phys. Chem. B* **2005**, *109*, 7046−7052.

(32) Kulik, H. J.; Marzari, N.; Correa, A. A.; Prendergast, D.; Schwegler, E.; Galli, G. Local Effects in the X-Ray Absorption Spectrum of Salt Water. *J. Phys. Chem. B* **2010**, *114*, 9594−9601.

(33) Waluyo, I.; Nordlund, D.; Bergmann, U.; Schlesinger, D.; Pettersson, L. G. M.; Nilsson, A. A Different View of Structure-Making and Structure-Breaking in Alkali Halide Aqueous Solutions through X-ray Absorption Spectroscopy. *J. Chem. Phys.* **2014**, *140*, 244506.

(34) Aziz, E. F.; Ottosson, N.; Eisebitt, S.; Eberhardt, W.; Winter, B.; et al. Cation-Specific Interactions with Carboxylate in Amino Acid and Acetate Aqueous: X-Ray Absorption and Ab Initio Calculations. *J. Phys. Chem. B* **2008**, *112*, 12567−12570.

(35) Fuchs, O.; Zharnikov, M.; Weinhardt, L.; Blum, M.; Weigand, M.; Zubavichus, Y.; Bär, M.; Maier, F.; Denlinger, J.; Heske, C.; et al.

Isotope and Temperature Effects in Liquid Water Probed by X-ray Absorption and Resonant X-ray Emission Spectroscopy. *Phys. Rev. Lett.* **2008**, *100*, 027801.

(36) Tokushima, T.; Harada, Y.; Takahashi, O.; Senba, Y.; Ohashi, H.; Pettersson, L. G. M.; Nilsson, A.; Shin, S. High Resolution X-Ray Emission Spectroscopy of Liquid Water: The Observation of Two Structural Motifs. *Chem. Phys. Lett.* **2008**, *460*, 387−400.

(37) Jeyachandran, Y. L.; Meyer, F.; Nagarajan, S.; Benkert, A.; Bär, M.; Blum, M.; Yang, W.; Reinert, F.; Heske, C.; Weinhardt, L.; et al. Ion-Solvation-Induced Molecular Reorganization in Liquid Water Probed by Resonant Inelastic Soft X - Ray Scattering. *J. Phys. Chem. Lett.* **2014**, *5*, 4143−4148.

(38) Yin, Z.; Rajkovic, I.; Thekku Veedu, S.; Deinert, S.; Raiser, D.; Jain, R.; Fukuzawa, H.; Wada, S.; Quevedo, W.; Kennedy, B.; et al. Ionic Solutions Probed by Resonant Inelastic X-ray Scattering. *Z. Phys. Chem.* **2015**, *229*, 1855−1867.

(39) Jeyachandran, Y. L.; Meyer, F.; Benkert, A.; Bär, M.; Blum, M.; Yang, W.; Reinert, F.; Heske, C.; Weinhardt, L.; Zharnikov, M. Investigation of the Ionic Hydration in Aqueous Salt Solutions by Soft X-Ray Emission Spectroscopy. *J. Phys. Chem. B* **2016**, *120*, 7687−7695.

(40) Petit, T.; Lange, K. M.; Conrad, G.; Yamamoto, K.; Schwanke, C.; Hodeck, K. F.; Dantz, M.; Brandenburg, T.; Suljoti, E.; Aziz, E. F. Probing Ion-Specific Effects on Aqueous Acetate Solutions: Ion Pairing versus Water Structure Modifications. *Struct. Dyn.* **2014**, *1*, 034901.

(41) Odelius, M. Molecular Dynamics Simulations of Fine Structure in Oxygen K-Edge X-ray Emission Spectra of Liquid Water and Ice. *Phys. Rev. B: Condens. Matter Mater. Phys.* **2009**, *79*, 144204.

(42) Marcus, Y. Effect of Ions on the Structure of Water: Structure Making and Breaking. *Chem. Rev.* **2009**, *109*, 1346−1370.

(43) Callahan, K. M.; Casillas-ituarte, N. N.; Roeselova, M.; Allen, H. C.; Tobias, D. J. Solvation of Magnesium Dication: Molecular Dynamics Simulation and Vibrational Spectroscopic Study of Magnesium Chloride in Aqueous Solutions. *J. Phys. Chem. A* **2010**, *114* (15), 5141−5148.

(44) Ohtaki, H.; Radnai, T. Structure and Dynamics of Hydrated Ions. *Chem. Rev.* **1993**, *93*, 1157−1204.

(45) Gråsjö, J.; Andersson, E.; Forsberg, J.; Aziz, E. F.; Brena, B.; Johansson, C.; Nordgren, J.; Duda, L.; Andersson, J.; Hennies, F.; et al. Electronic Structure of Water Molecules Confined in a Micelle Lattice. *J. Phys. Chem. B* **2009**, *113*, 8201−8205.

(46) Kunnus, K.; Rajkovic, I.; Schreck, S.; Quevedo, W.; Eckert, S.; Beye, M.; Suljoti, E.; Weniger, C.; Kalus, C.; Grübel, S.; et al. A Setup for Resonant Inelastic Soft X-ray Scattering on Liquids at Free Electron Laser Light Sources. *Rev. Sci. Instrum.* **2012**, *83*, 123109.

(47) Yin, Z.; Peters, H.-B.; Hahn, U.; Gonschior, J.; Mierwaldt, D.; Rajkovic, I.; Viefhaus, J.; Jooss, C.; Techert, S. An Endstation for Resonant Inelastic X-Ray Scattering Studies of Solid and Liquid Samples. *J. Synchrotron Radiat.* **2017**, *24*, 302−306.

(48) Hess, B.; Kutzner, C.; van der Spoel, D.; Lindahl, E. GROMACS 4: Algorithms for Highly Efficient, Load-Balanced, and Scalable Molecular Simulation. *J. Chem. Theory Comput.* **2008**, *4*, 435−447.

(49) Ferguson, D. M. Parameterization and Evaluation of a Flexible Water Model. *J. Comput. Chem.* **1995**, *16*, 501−511.

(50) Schuler, L. D.; Daura, X.; Van Gunsteren, W. F. An Improved GROMOS96 Force Field for Aliphatic Hydrocarbons in the Condensed Phase. *J. Comput. Chem.* **2001**, *22*, 1205−1218.

(51) Hariharan, P. C.; Pople, J. A. The Influence of Polarization Functions on Molecular Orbital Hydrogenation Energies. *Theor. Chim. Acta* **1973**, *28*, 213−222.

(52) Crawford, T. D.; Sherrill, C. D.; Valeev, E. F.; Fermann, J. T.; King, R. A.; Leininger, M. L.; Brown, S. T.; Janssen, C. L.; Seidl, E. T.; Kenny, J. P.; Allen, W. D. PSI3: An open-source Ab Initio electronic structure package. *J. Comput. Chem.* **2007**, *28*, 1610−1616.